UNIVERSITY OF BIRMINGHAM

University of Birmingham
College of Engineering and Physical Sciences

Department of Mechanical Engineering
School of Engineering

MSc Advanced Mechanical Engineering

Advanced Project

2015-16 Session

FINAL REPORT

Surname	SADAK
First Name	FERHAT
ID number	1602687
Supervisor's Name	Dr. Mozafar Saadat
Project Title	The vibrational analysis of the proposed micromanipulation system

Acknowledgement

I would like to express my deep and the sincerest gratitude to my advisor, Dr. Mozafar Saadat, for his magnificent guidance with strong patience, support and caring, and also giving me this opportunity to be a member of his group. His door was always open whenever I had questions regarding my dissertation.

I would like to thank to Doctoral Researcher Amir Hajiyavand, who has been a permanent source of inspiration throughout the dissertation by giving me inestimable suggestions.

Last but not least, I place a deep sense of gratitude to SADAK family, who has supported me morally during all my life.

Abstract

Intra Cytoplasmic Sperm Injection is one of the conventional methods in infertility treatment. In this method, a single sperm is injected into an oocyte with a direct injection under a microscope. However; there are several reasons which reduce the effects of the method significantly such as low success rates, long training, low efficiency, and contamination. Basically, this technique suffers from low efficiency and success rate. In the proposed system, stepper, delryne and servo motor have been employed on a platform and a glass holding micropipette was connected to the system. The design of the servo and stepper motors and the design of the micropipette cause vibration in the proposed system. Therefore, Vibrational analysis is essential in designing micromanipulators. These analyses will be considered for precision recognition. To analyze the total frequency of the proposed system, the micromanipulation system was divided into two main parts based on different type of frequencies occurred on the system. This work focuses on the lateral vibration of micro-pipette. Natural and resonance frequency of micropipette were calculated and validated. The effects of stepper and servo motor on micropipette displacement are also investigated and discusses in this report. In this paper, maximum deflection was obtained 700 Nanometer at the end of the micropipette, which is totally negligible in compare to the size of the cell. Furthermore, displacement of the micropipette caused by servo and stepper was initially 2um and after 35 seconds reached to constant equilibrium.

Index terms- micro-manipulation, Euler-Bernoulli, vibration analyses

1. Introduction

The World Health Organization reported, 48.5 million couple could not have the ability to have a baby in 2010. Also, it has been reported that 1.9 of the women aged 20-44 who wanted a child could not have their first live birth and 10.5 of the women population who had a baby before were unable to have the second baby after 5 years of trying [1].

There are few methods reported for the infertility treatments like IVF and Intracytoplasmic Sperm Injection (ICSI). Conventionally, cell injection was conducted manually via ICSI method by using two joysticks. In this technique; the single sperm is injected into an oocyte with a direct injection under a microscope, which increases the pregnancy rates as a higher possibility than other techniques, such as In Vitro Fertilization (IVF). Since in this approach, an oocyte is placed in Petri dish with several hundred sperms if possible, after that fertilization is aimed if a single sperm can successfully reach an oocyte. However; there are several reasons which reduce significantly the effects of the method used such as low success rates, long training, low efficiency, and contamination. Basically, human involvements lead to decrease the efficiency of the system.

Recently, several systems have been proposed to manipulate biological cells. Clement Leung et al. introduced microfluidic flow to manipulate the mouse embryos in three dimensional with minimum damages and high success rate up to 90% [2]. This system was also applied to obtain position and orientation of the polar body which is quite crucial. The polar body of an oocyte must be properly obtained for 3D micromanipulation applications since polar body consists of the copy of the genetic information of the oocyte. For that reason, Yu Sun et al. were used visual servoing and precision motion control together and a Hough transform was used to find the nuclei of embryos so that target destination can be obtained for visual servoing control system [3].

In conventional ICSI (Intracytoplasmic Sperm Injection), an embryologist operates manually since 1992. However, due to the fact that this method has human involvement, low success rates is the inevitable consequence of this technique. Therefore, Zhe Lu et al. was introduced a robotic ICSI system consisting of a cell holding device, motion control, and computer vision algorithm [4]. The vacuum-based holding device is introduced for immobilization. Tracking of the sperm head is mandatory for automation of sperm immobilization. Thus, a visual tracking algorithm was generated to track sperm head. In this study, sperm tail tracking was unsuccessful, when the sperms are in the air bubbles or large foreign particles. Considering this failure, the overall system operates with a success rate of 94.4%.

Recently, a new oocyte rotation method has been proposed based on the minimum rotation force by Qili Zhao et al. [5]. In this technique, minimum rotation force calculated was used to perform robotic rotation for the oocyte with minimum rotation deformation with the success rate of 93.3%. This technique has less cell deformation, higher control accuracy, and less human involvement. However, In this technique, the required force depends on the cell

properties and also it is extremely hard to calculate the required force for each individual due to a negative pressure of the holding pipette [6].

Optical tweezers are used for 3-dimensional rotation of microscopic objects by using pulsed near infrared laser beams which cause a tangential force on the object in order to rotate [7]. In this case, the size of the object and rotating a cell about one axis is considered as limitations [8]. Moreover, the cells are exposed to direct laser beam causing to damage the cells and makes the system effectiveness. Therefore, Thakur et al. combined the optical tweezers technology with an image guided robotics technique in order to have indirect manipulation the cells without damage [9] .

On the reported researches, there is no analysis of vibration as it is one of the main factors in the outcome of precision in manipulation.

Automated micromanipulation system has the advantages of high speed and precision, however, this system is required vibration analyze since vibration can cause either dropping or damaging the biological cell. On this purpose, Avci et al. [10] used a high-speed camera to observe oscillation . After that Fast Fourier Transformation is used to analyze the oscillation and get the frequencies within the oscillations. Finally, the applicability of real-time feedback control was searched on vibration analyzes. Similar work also has been done by Avci et al. [11]. In proposed work, the stiffness of the system was increased with the feedforward control, therefore vibration amplitude and duration were decreased.

Despite, piezo actuator is widely used in ICSI operation, using piezoelectric actuator causes lateral vibration at the tip of the micropipette in the intracytoplasmic sperm injection (ICSI) process. Mehdi Karrzar-Jeddi et al. suggest a solution for compensation of lateral vibration in ICSI operation [12]. An analytical solution was generated to realize dynamic behavior of micropipette by using Euler-Bernoulli beam theory with empty and mercury filled pipette's tip. It has been realized the fluid damping effect has a role in vibration analysis since shear force and displacement with filled mercury was higher than empty micro pipette's tip. However, Ediz and Olgac investigated the mercury filled micropipette in ICSI operation, and it is believed that natural frequencies of micropipette are reduced by increasing the mercury mass loading[13]. Fluid damping effect is not the only concern that needs to be investigated. Kong et al. solved simple supported and cantilever Euler-Bernoulli beam analytically by considering initial and boundary conditions, and that the obtained natural frequency of beams is highly dependent on the size of beams[14]. Analytical solution Kong et al. derivation is quite important for the micron or sub-micron size beams to understand the stiffness of the micropipette since if the micropipette is not stiff enough, vibration analyses need to be checked immediately to increase the success rate in terms of positioning oocyte accurately.

Although reducing the vibration is an initial purpose in the literature, however, also piercing force should be effective enough to penetrate the cell membrane by helping lateral vibration [15] which has a significant role in ICSI operation since the amplitude of lateral vibration is larger than

axial vibration in cell membrane piercing process [16]. Vibrations have been caused by the different source of vibration. In each system, these sources play important roles in the vibrational analysis. Consequently, these sources are going to be described and explained in the following section.

Servo and stepper motor are widely used in micromanipulation system in order to build system position. Even though stepper motor can find system position faster and more accurate than servo motor, however, it is quite expensive. Furthermore, there is a difference between servo and stepper motor because while typical servo motor has 2-8 poles, typical stepper motor has 25-100 poles. The stepper motor has a lot of torque at a lower speed while servo motor has a flat torque which is related to the number of poles that each motor has.

Misalignment of the rotor in the stepper motor which magnetic field keep in a particular position will be a cause of vibration because of the fact that rotor will feel the torque. Therefore, if we try to keep in the alignment, the rotor will begin to move toward alignment until it reaches because when it reaches the alignment it cannot stop and it overshoots because of its own inertia [17].

Fast speed grasping of a biological cell is a desirable feature of automated micromanipulation system. That is the reason why servo motor is used to control the micropipettes. Typical micromanipulation system has 0.1 mm/s speed which almost does not cause vibration. However, at high speed which is normally 2.3 mm/s causes vibration. In this case, there is acceleration for micropipette to move toward to cell and also decelerating to stop itself. The changes between accelerating and decelerating cause usually the vibration [18]. Obviously, at high speed, the changes will be greater than normal speed and therefore more vibration. It should be pointed out that vibration can cause the dropping or damaging of the biological cells.

As is well known, high positioning accuracy is an inevitable desire of micromanipulation system. To obtain high positioning accuracy, the first thing has to get through the environmental noise. On this purpose, environmental isolation platform can be a solution for micro-robotic systems [19].

The vibrational analysis is essential in designing micromanipulators. These analyses will be considered for precision recognition. In this purpose, M. Boudaoud et al. searched the source of vibration[20]. In this research, a cantilever is used to model it dynamically to find the dynamic response of the model under environmental noise by using finite difference formulation of the Euler-Bernoulli. Tip vibration of an end effector can be simulated using Matlab/Simulink software.

After that, experimentally, four cantilevers were used in different length, width, thickness, stiffness and resonance to show the effect of the environmental noise on the cantilever. In the experiment, acoustic noise is recorded by microphone and ground motion is transferred to the base of the cantilever and recorded by using laser interferometer to measure the vibration.

Isolation table was used to reduce the ground motion. In this case, the cantilever is subject to ground motion and acoustic noise.

As a consequence of work, simulation and experimental data are totally matched. After that, the effect of noise and ground motion on the cantilevers were analyzed. On this purpose, the horizontal vibration on vibration isolation table was measured in micromanipulation room by using laser interferometer during one day. Apart from that, the acoustic noise was measured during the day by taking low and high human activity into account.

Under this experimental condition, acoustic noise has been measured in the micromanipulation room with low and high human activity. It can be concluded that human activity has a significant effect on acoustic noise considering as a source of vibration.

Before and after the experiment for each cantilever, the frequency was calculated and compared. As a result of the comparison, it has been found that there is a significant difference between both experiments in frequency in low human activity. The reason behind of this is to use vibration isolation table.

To show the single effect of unidirectional acoustic noise, an experiment is made in an anechoic chamber and all system is transferred into the anechoic chamber which is covered by rubberized material foam and almost no vibration from the ground. The data is demonstrating that the amount of frequency in acoustic noise in the micromanipulation room with low human activity was higher than the frequency of acoustic noise in the anechoic chamber.

In conclusion, environmental noise which consists of ground motion and acoustic noise should be evaluated as significant vibration source in micromanipulation systems. In this direction, an appropriate controller for noise rejection can be a solution [21][20]. Multi noise isolation platform can be considered as a solution to get rid of ground motion , however, these platforms have limited work volume and if we need a large working volume, that would be a restriction for the system [22][20].

In this report, first of all, vibration analyses for micropipette were discussed analytically in the proposed system to recognize the amount of vibration occurs during the operation. The secondly, the effect of the amount of deflection and displacement caused by servo and stepper was presented. The contribution of the paper, present the behavior of the micropipette under operation by considering crucial factors. Last but not least, the initial purpose of vibration analysis is employed to verify the stiffness of the proposed system. In the paper, the micromanipulation system was divided into two main parts for analyzing the total frequency of the system. Natural frequency and noises of micropipette were calculated and validated in the methodology section. The result of natural frequency and vibrational noises have been discussed later in the result and discussion part. Later on, the amount of natural frequency, displacement, and deflection of the micropipette and the vibrational noise was obtained for the system and concluded in the conclusion part.

2. Methodology

This section discusses the methods of analyzing the vibration for the proposed system. This analysis supports the proposed design and investigates the amount of vibration which finally effect on the accuracy of the system. As the application of the system is in micro-manipulation of the biological samples like a cell, so it is important to minimize the misallocating of the end effector. The following figure shows the schematic sketch of one of the manipulators and the system design of it.

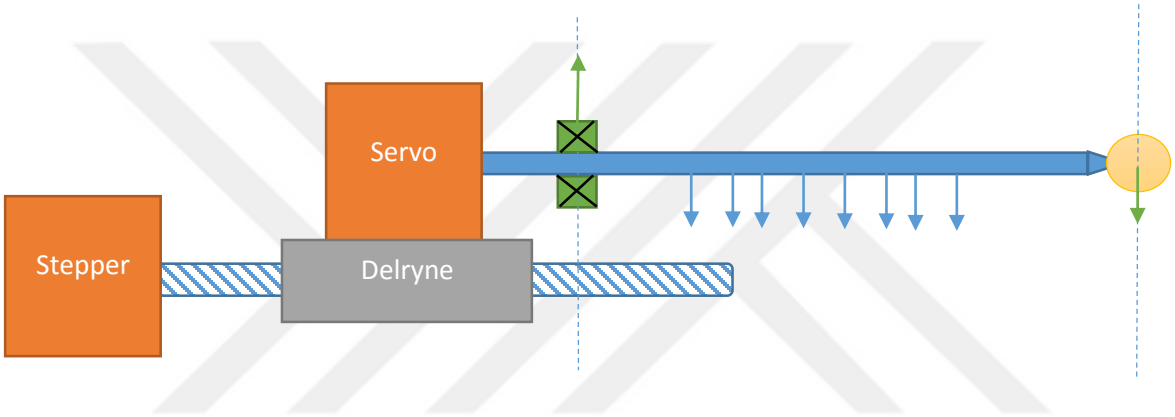

Figure 1 Schematic sketch of micro pipette and system design

In the proposed system, stepper, delryne and servo motor have been employed on a platform and a glass holding micropipette was connected to the system. This system is manipulating a single cell to the desired location. The stepper motor connects to the lead screw which has a responsibility of controlling the linear motion of the delryne. Servo motor which is assembled on the delryne has the responsibility of controlling the circular motion of the micropipette along its center line. The micropipette is fixed on the servo motor and has a support of bearing to avoid more vibrating.

This work focuses on lateral vibration rather than axial vibration since experimental and analytical results suggests that lateral vibration is much more crucial in terms of investigation of holding micropipette's vibration in comparison with axial oscillations [12][23] since lateral vibration is much more effective than axial vibration in terms of piercing cell membrane operation [16][15]. Furthermore, resonance frequency which was created by external force was calculated for stepper and servo motor individually. Displacement of micropipette which was caused by stepper and servo motor was also obtained.

In the proposed system, the total frequency of the system has been calculated by separating the system into 2 parts which are servo and stepper motor's resonance frequency and micropipette's natural frequency. Bearings were used to support the micropipette from bending.

In the system, glass micropipette was assumed as a beam with one fixed and one free end. To predict vibration of the system, lateral vibration analysis was considered for the micropipette. Lateral vibration occurs due to the external loads, unbalance and instability which are existed in the proposed system due to servo and stepper motors and very thin glass micropipette.

Next section will focus on the type of frequencies. These frequencies have the main effect on the noise and vibration analysis of the system.

2.1 Type of frequencies

Regarding types of frequencies, there are two main reasons which for analyzing the frequency and vibrations which are natural frequency and resonance. The natural frequency is a frequency at which it oscillates itself because of own property such as flexibility, mass etc. Therefore, the natural frequency is not a material property, it is a system property. If one of the natural frequency is equal to the resonance frequency, which means that the system will have over vibration.

The resonance frequency is a different phenomenon since it occurs if there is an external force such as stepper and servo motor's torques in proposed system. The system is exerted by external force periodically at the same period of one of the natural frequencies of the system. In the system, 4 modes of natural frequency were calculated.

2.2 Natural frequency of micropipette analytically in four modes

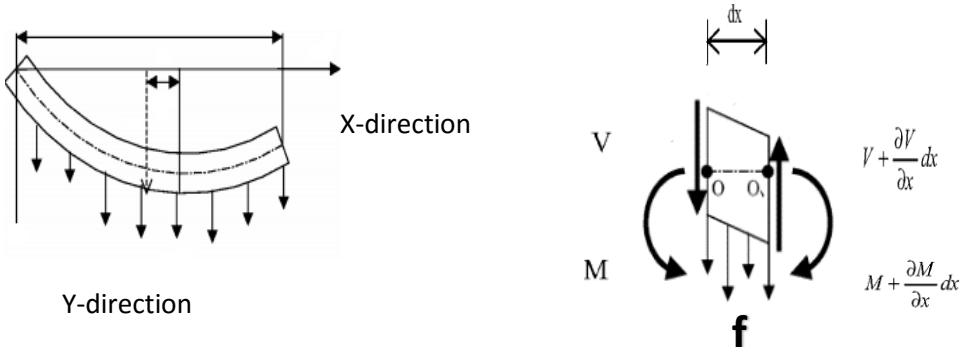

Figure 2. a. Lateral vibration of a beam b. Free body diagram

In this part, the analytical equations have been developed to analyses the deflection, natural and resonance frequencies. As it is shown in free body diagram in figure 2, the inertia force acting on a micropipette can be written;

$$\rho A(x)dx \ \frac{\partial^2 w}{\partial t^2}(x,t) \tag{1}$$

Where ρ is the mass density and A(x) is the cross-sectional area of micropipette. Basically, this formula is coming from Newton's second law.

Later on, with respect to the free body diagram, figure 2b, moment and force equation of motion is written independently in order to obtain the equation of motion of micropipette. By using that formula, forced lateral vibration along non-uniform micropipette can be obtained.

First of all, force equilibrium in the y-direction using the free body diagram can be written as;

$$-(V + dV) + f(x,t)dx + V = \rho A(x)dx \ \frac{\partial^2 w}{\partial t^2}(x,t) \tag{2}$$

Moment equation about x-axis to 'O' point in free body diagram can be expressed as;

$$(M + dM) - (V + dV)dx + f(x,t)dx.\frac{dx}{2} - M = 0 \tag{3}$$

Where;

$$dV = \frac{\partial V}{\partial x}dx \quad and \quad dM = \frac{\partial M}{\partial x}dx \tag{4}$$

That equation is applied to equation 2 and 3 and equations can be written as;

$$-\frac{\partial V}{\partial x}(x,t) + f(x,t) = \rho A(x)\frac{\partial^2 w}{\partial t^2}(x,t) \tag{5}$$

$$\frac{\partial M}{\partial x}(x,t) - V(x,t) = 0 \tag{6}$$

When the relation between force and bending moment used, which is $V = \frac{\partial M}{\partial x}$

equation 5 and 6 become;

$$-\frac{\partial^2 M}{\partial x^2}(x,t) + f(x,t) = \rho A(x)\ \frac{\partial^2 w}{\partial t^2}(x,t) \tag{7}$$

By using force and bending moment relation, equation 7 was obtained since equation 6 canceled itself out. As a result, the equation of motion was obtained. However, still changing bending momentum with respect to time along micropipette should be written in the form of deflection along micropipette with respect to time.

To solve that equation, a relationship between bending moment and deflection is essential on micropipette which is called Euler-Bernoulli thin beam theory.

$$M(x,t) = \ EI(x)\frac{\partial^2 w}{\partial x^2}(x,t) \tag{8}$$

Where E is Young's modulus and I is the moment of inertia of micropipette. when we substitute the equation 8 into the equation 7, a new equation can be written as;

$$\frac{\partial^2}{\partial x^2}\left[EI(x)\frac{\partial^2 w}{\partial x^2}(x,t)\right] + \rho A(x)\frac{\partial^2 w}{\partial t^2}(x,t) = f(x,t) \quad (9)$$

That equation shows that how does the micropipette behavior under force in order to observe the forced lateral vibration along micropipette. If we distribute $\frac{\partial^2}{\partial x^2}$ term , the equation is reduced to;

$$EI\frac{\partial^4 w}{\partial x^2}(x,t) + \rho A(x)\frac{\partial^2 w}{\partial t^2}(x,t) = f(x,t) \quad (10)$$

Equation 10 presents that the deflection behavior of micropipette under distributed load f (x, t) along micropipette. Due to the fact that proposed system generates lateral vibration along micropipette (free vibration), distributed load is taken as '0' which makes generated equation 10 homogenous partial differential equation which is;

$$EI\frac{\partial^4 w}{\partial x^2}(x,t) + \rho A(x)\frac{\partial^2 w}{\partial t^2}(x,t) = 0 \quad (11)$$

As it is obtained in equation 11, we have fourth order derivative with respect to x and second-order derivative with respect to time. Therefore, in order to obtain the deflection w (x, t), 4 boundary conditions and 2 initial conditions are needed. These conditions are stated in table 1.

Table 1. Boundary and Initial conditions of micropipette

Boundary conditions of micropipette	**Initial conditions of micropipette**
$w(0,t) = 0$ (Fixed end)	$w(x,0) = 0$
$\frac{\partial w(0,t)}{\partial x} = 0$ (Fixed end)	$\frac{\partial w(x,0)}{\partial t} = 0$
$\frac{\partial^2 w(l,t)}{\partial x^2} = 0$ (Free end)	
$\frac{\partial^3 w(l,t)}{\partial x^3} = 0$ (Free end)	

In terms of natural frequencies of the micropipette, the respective solution with respect to end condition of the micropipette is presented below. The free end is assumed since oocyte almost does not apply force to the tip of the micropipette.

The characteristic of micropipette W (x) in 4 modes should be determined in 4 modes to see the natural frequency of micropipette and validate from the literature[23].

Mode Shape (Normal Function) is stated below as a general solution.

$$W_n(x) = C_n[sin\beta_n x - sin\, h\beta_n x - \alpha_n(cos\beta_n x - cos\, h\beta_n x)] \quad (12)$$

Where;

$$\alpha_n = \frac{sin\beta_n l + sin\, h\beta_n l}{cos\beta_n l + cos\, h\beta_n l} \quad (13)$$

In or to obtain β_n and C_n , common boundary conditions of micro pipette are used. Therefore, bending moment and shear force are taken as '0'. This boundary condition applied to a beam which is fixed on one end and free on the other end.

C1, C2, C3, C4 are constants and β1, β2, β3, β4 are the eigenvalues and all values are determined from boundary conditions of the micropipette. Due to the fact that the micropipette is one and fixed and the other end is free, table 2, is used to compute the natural frequency of the micropipette in 4 modes. Natural frequency of micropipette is stated as;

$$w = \beta^2\sqrt{\frac{EI}{\rho A}} = (\beta l)^2\sqrt{\frac{EI}{\rho A l^4}} \quad (14)$$

Table 2. Eigenvalues in 4 modes[12]

β1.l	1.875104
β2.l	4.694091
β3.l	7.854757
β4.l	10.995541

w1, w2, w3 and w4 are found in 4 modes and validated from the literature[23].

2.3 Resonance Frequency of Servo and Stepper motor

As it is mentioned before, correct selection of stepper and servo motors are crucial in micromanipulation system. Particularly, servo and stepper types have a big role in producing vibration. Even the number of pole pairs which stepper and servo motor have is quite important for the calculation of resonance frequency of the motors, which is stated in the formula 15. Eccentricity is the differences between the amount of roll deviation that servo and stepper motors produce from being faultless circular. Zero eccentricity is desirable, however, it never goes to zero in reality. Eccentricity is the main source of vibration in these type of motors. That eccentricity can be dynamics or static on electromagnetic performance [24][25]. All these reasons cause vibration since it has been produced extra external force leading to extra resonance frequency for the system. This extra resonance frequency causes more displacement for micropipette.

The resonance frequency of servo and stepper motor is calculated by equation 15. With respect to specification of the servo and stepper motors, resonance frequency was calculated for each motor.

Motor resonance frequency can be obtained as follows:

$$f = \frac{100}{2\pi}\sqrt{\frac{2 \cdot p \cdot M_h}{J_r}} \quad (15)$$

Where f is motor resonance frequency (Hz), p is a number of pole pairs (dimensionless), M_h is holding torque (N X m), J_r is rotor inertia (kg X m2).

After Completion of resonance frequency calculation, micropipette displacement calculation for stepper and servo motor were developed by helping of equation 16 in order to observe the effect of motors on micropipette during 60 seconds.

$$Pipette\ position(t) = Ke^{\zeta wt}\ sin\left(w\sqrt{1-\zeta^2}\ t\right) \quad (16)$$

Where K is a scaling factor, w is the resonant frequency in radians and ζ is the damping factor.

Next section will focus of the results obtained from the developed analytical modeling for natural and resonance frequencies and discuss the effect of these results on the system outcome.

3. Results and Discussions

In this section, the obtained results of the analytical modeling are discussed. The results demonstrate the deflection of the micropipette and natural frequency of it as well as frequency analyses based on the employed motors.

Figure 3 shows deflection along micropipette. Free vibration does not have any effect on the micropipette natural frequency so it should be pointed out that partial differential equation was equaled to zero because of the fact that we have free vibration. Distance from the bearings supporting the micropipette to reduce vibration to the tip of micropipette was 0.05 meter. Figure 3, illustrates that the micro pipette's deflection is almost linear and the deflection at the tip of the micropipette has the highest rate. The deflection rate from fixed point until 0.005 meter is almost remained constant due to the fact that it is quite close to bearings which plays a support role. To add more supports in order to reduce the deflection can be a practical solution in the future, although the amount of the deflection is less than a threshold to be a significant concern. For instance, one more bearing can be assembled to the middle of the micropipette. The design of the micropipette is also crucial for the precision of the system. The mechanical solution of the micropipette is considered in terms of thickness and mass of the micropipette by using equation 17 and 18, and equations show that the thicker and heavier micropipette has less natural frequencies [11].

$$f_n \approx \sqrt{\frac{EI}{mL^4}} \quad (17)$$

Where; f_n is natural frequency, E is elastics modulus of micro pipette, I stands for the moment of inertia, m is applied force and L presents the length of micro pipette.

$$\delta_{max} \approx \frac{wL^4}{EI} \quad (18)$$

Where; w is applied force, δ presents the maximum deflection of the micropipette.

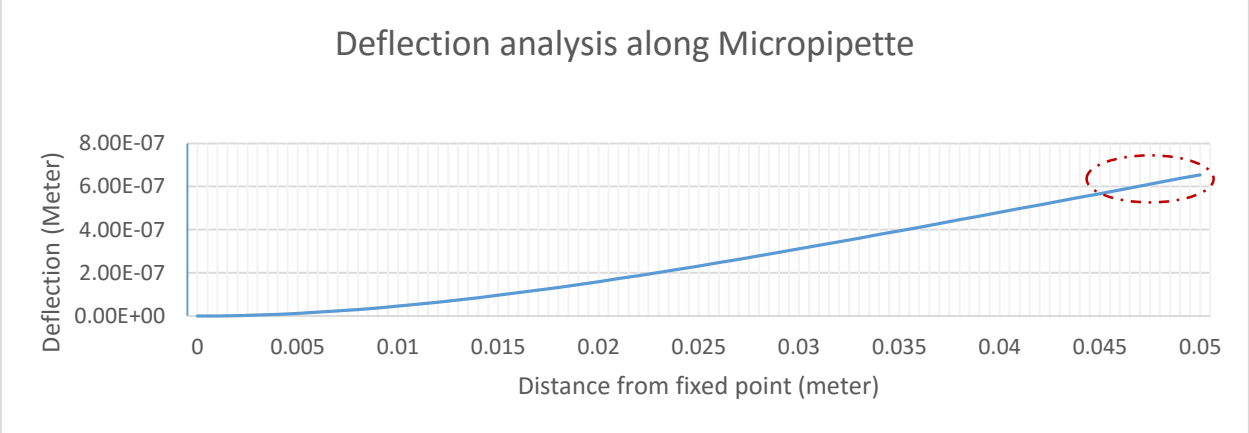

Figure 3. Deflection analysis results along micro pipette

The indicated area with the red dotted line shows the maximum deflection of the pipette which is at the tip of the pipette. The maximum deflection is 700 Nanometer which is totally negligible in compare to the size of the cell.

After deflection was calculated and plotted, equation 14 was used to obtain four modes of natural frequencies and validated from literature[23] as it is shown in table 3.

Table 3. Comparison of natural frequencies between developed model and literature

Natural Frequency for pipette (Hz)			
Modes	Based on developed method	Based on Literature[23]	Error
Mode 1	9.99	10	0%
Mode 2	62.64	63	1%
Mode 3	175.41	175	0%
Mode4	343.75	341	1%

The obtained results demonstrate that the analytical results are quite close to literature' results with a negligible error. The paper uses the same micropipette and it was expected to get close results.

There are 4 modes of natural frequencies. There are many sources effect on the vibration such as unstable micropipette due to its weight, oocyte weight [26] and fluid inside micropipette which causes the vibrations changes along the micropipette.

Apart from that, the effect of servo and stepper motor on the micropipette's vibration will be shown analytically in the following part. These motors lead to changeable vibration along micropipette. As it is stated before, also, ground motion and acoustic will affect the micromanipulation system and each source of vibration will have an own frequency. Sometimes, while these different type of sources effect vibration of the micropipette as a group, sometimes not. Therefore, micropipette's oscillation will be unstable during operation. It is quite hard to imagine the shape of vibration. For this reason, it is better to evaluate the system in four different modes. In the light of vibration variation, therefore, the micro pipette's natural frequencies were evaluated in 4 modes which were stated in figure 4.

Figure 4 illustrates different modes of frequencies in the bar chart. The blue bars show the obtained results and those values were validated from literature which is orange bars [23].

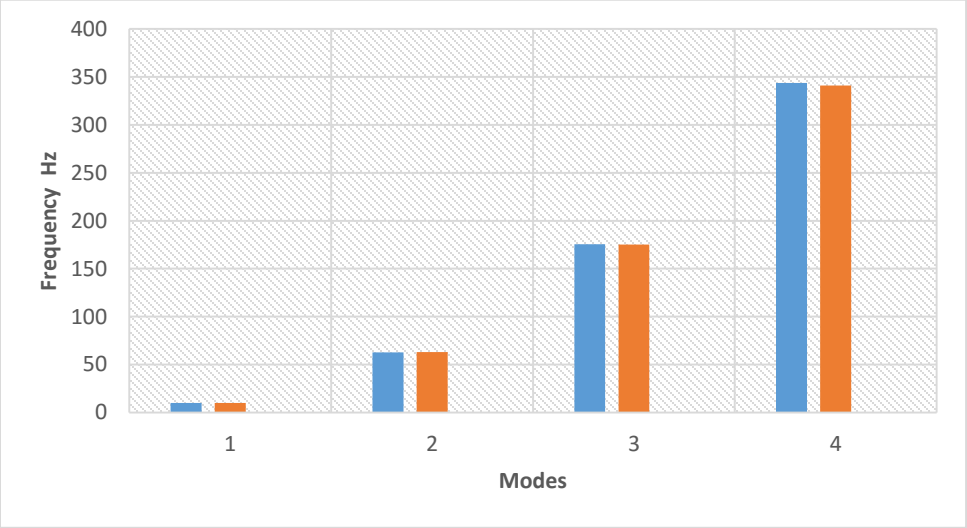

Figure 4 Four modes of frequency comparison

Figure 5 shows significant mode difference analysis which demonstrates the variance between mode 1 and mode 4. As it is presented that the frequency differences at 8^{th} seconds is totally opposite between modes. While mode 1 is increasing sharply, mode 4 is decreasing. To be precise, there is a sharp fluctuation between mode 1 and mode 4 during 49 seconds. That is the analytic evidence to understand clearly the difference of mode of frequencies.

Figure 5. Variance between Mode 1 and Mode 4

Resonance frequency caused by external forces was computed by using equation 15 for servo and stepper motors separately and results were stated in table 4 in Hz. The stepper motor has less resonance frequency than servo motor since servo motor has low rotor inertia and high holding torque. The initial purpose of calculating resonance frequencies of motors is to add them to the natural frequency of micropipette and obtain all vibration of the proposed system. The second purpose is to see the impact of resonance frequencies of servo and stepper motor on the behavior of micropipette during 60 seconds in displacement. The Very interesting phenomenon was released during 60 seconds.

Table 4. Resonance frequency of servo and stepper motor

External sources	Resonance Frequency (Hz)
Stepper motor	4.898685787
Servo motor	6.386833751

Figure 6a and 6b clearly shows that the displacement of micropipette caused by servo and stepper motor. First of all, in terms of the stepper motor, once we turn on the micromanipulation system, it will oscillate up to 2 µm between first few seconds which starts immediately after 0.1 seconds and the displacement is going down gradually until 25 seconds although displacement between 20^{th} and 25^{th} seconds are very minor. The major vibration occurs in first 20 seconds after the start of the motors. If the manipulation operates in this time interval, then it may end with low accuracy in terms of cell delivery and cell operation and that may cause some un-predicted damages to the cell.

As the displacement graphs illustrate, the amount of the vibration were dramatically decreased after 15 seconds. Also, the amount of the vibration for servo stops after 20 seconds but the stepper motor still causes some vibrations till 35 seconds as indicates by red dashed line.

It should be noted that the amount of the vibration for both servo and stepper is not considerably high that affect too much on the precision after 15 seconds.

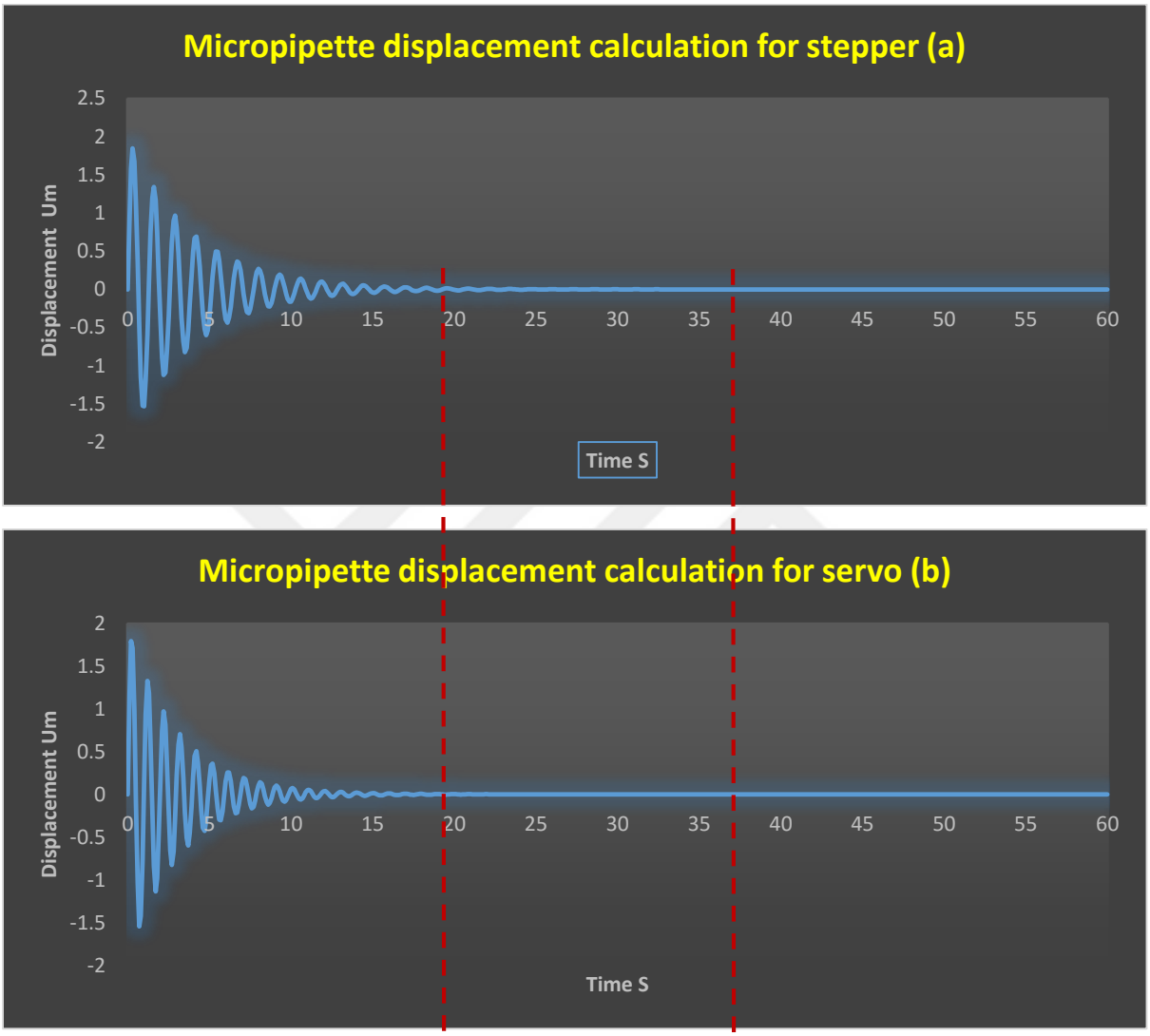

Figure 6 a. Displacement of micropipette for stepper b. Displacement of micropipette for servo

4. Conclusion

The aim of this work is to observe the vibration behavior of micropipette in a complex system. For this reason, natural frequencies of micropipette were calculated and plotted along the micropipette by using fundamental Euler-Bernoulli thin beam theory. Stepper and servo motors have an impact on micropipette during the operation in terms of the resonance frequency. After the servo and stepper motor's resonance frequency was calculated, the total frequency of the micromanipulation system was obtained and evaluated.

Analytical solution of the micro pipette's deflection was derived and the deflection was found almost linear and the deflection at the tip of the micropipette has the highest rate along micropipette although the amount of the deflection is less than a threshold to be a significant concern. Because the maximum deflection is 700 Nanometer at the top of the micropipette, which is totally negligible in compare to the size of the cell.

The requirement of investigation micropipette's natural frequencies in 4 modes was realized since it is hard to imagine the shape of vibration during operation as it is shown figure 4. Natural frequencies of the micropipette in 4 modes were investigated and validated with a negligible error.

Furthermore, the pattern of displacement during 60 seconds was plotted to show the effect of motors on micro pipette's displacement. We can conclude from this information, displacement on the micropipette caused by servo and stepper remained constant as from almost 20th second, however, for servo motor, displacement still goes up and down slightly until 35^{th} seconds. Therefore, if the operation is started after 35th seconds, the displacement decreases by 2 um and high accuracy is achieved.

As a future work, the obtained results will feed to optimize the design in a way to have less vibration. Although the amount of Vibration is not so much that effect on the manipulation. Next step of this analysis should be considering the whole operation in a FE analysis software and also do the real time experiment and examine the vibration using vision detection methods and compare to the demonstrated results.

References

[1] M. N. Mascarenhas, S. R. Flaxman, T. Boerma, S. Vanderpoel, and G. A. Stevens, "National, Regional, and Global Trends in Infertility Prevalence Since 1990: A Systematic Analysis of 277 Health Surveys," *PLoS Med.*, vol. 9, no. 12, p. e1001356, Dec. 2012.

[2] C. Leung, Z. Lu, X. P. Zhang, and Y. Sun, "Three-dimensional rotation of mouse embryos," *IEEE Trans. Biomed. Eng.*, vol. 59, no. 4, pp. 1049–1056, 2012.

[3] Y. Sun and B. J. Nelson, "Biological cell injection using an autonomous microrobotic system," *Int. J. Rob. Res.*, vol. 21, no. 10–11, pp. 861–868, 2002.

[4] Z. Lu, X. Zhang, C. Leung, N. Esfandiari, R. F. Casper, and Y. Sun, "Robotic ICSI (Intracytoplasmic Sperm Injection)," *IEEE Trans. Biomed. Eng.*, vol. 58, no. 7, pp. 2102–2108, 2011.

[5] Q. Zhao, M. Sun, M. Cui, J. Yu, Y. Qin, and X. Zhao, "Robotic Cell Rotation Based on the Minimum Rotation Force," *IEEE Trans. Autom. Sci. Eng.*, vol. 12, no. 4, pp. 1504–1515, 2015.

[6] Z. Wang, C. Feng, R. Muruganandam, J. Mathew, P. C. Wong, W. T. Ang, S. Yih, M. Tan, and W. T. Latt, "A Fully Automated Robotic System for Three-dimensional Cell Rotation," pp. 1707–1712, 2016.

[7] S. K. Mohanty and P. K. Gupta, "Laser-assisted three-dimensional rotation of microscopic

objects," *Rev. Sci. Instrum.*, vol. 75, no. 7, pp. 2320–2322, 2004.

[8] E. P. Y. Chiou and M. C. Wu, "Optoelectronic Tweezers," *Micro/Nano Technol. Syst. Biomed. Appl. Microfluid. Opt. Surf. Chem.*, no. 1, 2010.

[9] A. Thakur, S. Chowdhury, P. Vec, C. Wang, W. Losert, and S. K. Gupta, "Indirect pushing based automated micromanipulation of biological cells using optical tweezers," *Int. J. Rob. Res.*, vol. 33, no. 8, pp. 1098–1111, 2014.

[10] E. Avci, C.-N. Nguyen, K. Ohara, Y. Mae, T. Arai, and C. Gobel, "Vibration analysis of microhand for high speed single cell manipulation," *2012 IEEE Int. Conf. Mechatronics Autom.*, pp. 75–80, 2012.

[11] E. Avci, C. Nguyen, K. Ohara, M. Kojima, Y. Mae, and T. Arai, "Towards High Speed Automated Micromanipulation," pp. 1718–1723, 2013.

[12] M. Karzar-Jeddi, N. Olgac, and T. H. Fan, "Dynamic response of micropipettes during piezo-assisted intracytoplasmic sperm injection," *Phys. Rev. E - Stat. Nonlinear, Soft Matter Phys.*, vol. 84, no. 4, pp. 1–9, 2011.

[13] K. Ediz and N. Olgac, "Effect of Mercury Column on the Microdynamics of the Piezo -Driven Pipettes," *J. Biomech. Eng.*, vol. 127, no. 3, pp. 531–535, 2005.

[14] S. Kong, S. Zhou, Z. Nie, and K. Wang, "The size-dependent natural frequency of Bernoulli-Euler micro-beams," *Int. J. Eng. Sci.*, vol. 46, no. 5, pp. 427–437, 2008.

[15] Z. N. Wang, W. T. Ang, S. Zhao, and T. J. Teo, "Application of lateral oscillating piezo-driven micropipette in embryo biopsy for pre-implantation genetic diagnosis," *2014 13th Int. Conf. Control Autom. Robot. Vision, ICARCV 2014*, vol. 2014, no. December, pp. 1218–1223, 1997.

[16] Z. Wang, S. Zhao, and W. T. Ang, "Beneficial micropipette oscillation in vision-guided piezo-assisted ICSI," *2013 IEEE Int. Conf. Robot. Biomimetics, ROBIO 2013*, no. December, pp. 1665–1670, 2013.

[17] D. Gorupec, "Stepper motor vibrations," 2014.

[18] E. Avci, "High-Speed Automated Micromanipulation System with Multi-Scalability," Osaka University, Graduate School of Engineering Science, 2013.

[19] C. J. H. Brenan, P. G. Charette, and I. W. Hunter, "Environmental isolation platform for microrobot system development," *Rev. Sci. Instrum.*, vol. 63, no. 6, pp. 3492–3498, 1992.

[20] M. Boudaoud, Y. Haddab, Y. Le Gorrec, and P. Lutz, "Noise characterization in millimeter sized micromanipulation systems," *Mechatronics*, vol. 21, no. 6, pp. 1087–1097, 2011.

[21] M. Rakotondrabe, K. Rabenorosoa, and N. Chaillet, "Characterization , modeling and robust control of a nonlinear 2 -dof piezocantilever for micromanipulation / microassembly," pp. 767–774, 2009.

[22] B. Tamadazte, N. Le Fort-Piat, S. Dembélé, and G. Fortier, "Robotic micromanipulation for microassembly: Modelling by sequencial function chart and achievement by multiple scale visual servoings," *J. Micro-Nano Mechatronics*, vol. 5, no. 1, pp. 1–14, 2009.

[23] K. Ediz and N. Olgac, "Microdynamics of the piezo-driven pipettes in ICSI," *IEEE Trans. Biomed. Eng.*, vol. 51, no. 7, pp. 1262–1268, 2004.

[24] S. Jia, R. Qu, J. Li, Z. Fu, H. Chen, and L. Wu, “Analysis of FSCW SPM servo motor with static, dynamic and mixed eccentricity in aspects of radial force and vibration,” *2014 IEEE Energy Convers. Congr. Expo. ECCE 2014*, pp. 1745–1753, 2014.

[25] Z. Q. Zhu, L. J. Wu, and M. L. Mohd Jamil, “Distortion of back-EMF and torque of PM brushless machines due to eccentricity,” *IEEE Trans. Magn.*, vol. 49, no. 8, pp. 4927–4936, 2013.

[26] G. J. Macchi, M. P??jaro, M. I. Militelli, N. Radovani, and L. Rivas, “Influence of size, age and maternal condition on the oocyte dry weight of Argentine hake (Merluccius hubbsi),” *Fish. Res.*, vol. 80, no. 2–3, pp. 345–349, 2006.